



ELSEVIER

Contents lists available at ScienceDirect

Biosensors and Bioelectronics

journal homepage: www.elsevier.com/locate/bios

Magnetic graphene oxide-supported hemin as peroxidase probe for sensitive detection of thiols in extracts of cancer cells

Sai Bi^{a,b,*}, Tingting Zhao^b, Xiaoqiang Jia^b, Peng He^b^a Shandong Provincial Key Laboratory of Detection Technology of Tumor Markers, School of Chemistry and Chemical Engineering, Linyi University, Linyi 276005, China^b Key Laboratory of Sensor Analysis of Tumor Marker, Ministry of Education, College of Chemistry and Molecular Engineering, Qingdao University of Science and Technology, Qingdao 266042, China

ARTICLE INFO

Article history:

Received 17 October 2013

Received in revised form

16 January 2014

Accepted 17 January 2014

Available online 8 February 2014

Keywords:

Artificial enzyme mimetic

Colorimetry

Graphene oxide (GO)

Probe

Thiols

ABSTRACT

Magnetic graphene oxide (GO)–hemin probes containing disulfide bonds are simply and effectively synthesized through amide reaction to covalently link magnetic particles to GO surface and π – π stacking interaction between hemin and GO to immobilize hemin on GO. Based on the strong nucleophilicity of sulfhydryl, we have developed a colorimetric detection system for thiols by using glutathione (GSH) as a model analyte. Upon the introduction of GSH to the fabricated magnetic particle (MP)–GO–hemin probes, the disulfides can be readily reduced by thiols, resulting in the release of GO–hemin hybrids to solution. Due to the existence of hemin on GO surface, the released GO–hemin that has the intrinsic peroxidase-like activity can catalyze the oxidation of ABTS^{2-} by H_2O_2 to form the colored radical product $\text{ABTS}^{\cdot-}$. A broad linear dynamic range of 10^{-10} M to 10^{-6} M GSH is achieved with a detection limit of 8.2×10^{-11} M (3σ). Moreover, the new probe is successfully applied to the detection of non-protein thiols and protein thiols in the extracts of Ramos cells, which shows favorable correlation with the results obtained by electrochemical method. In addition, the MP–GO–hemin probe can detect non-protein thiols in Ramos extracts as low as 500 cells. In this assay, the prepared MP–GO–hemin conjugates are thoroughly characterized by SEM, AFM, UV–Vis, FT–IR, and Raman spectroscopy.

© 2014 Elsevier B.V. All rights reserved.

1. Introduction

Graphene with a one-atom thickness and two-dimensional plane structure has attracted considerable attention due to its unique physical, chemical, and mechanical properties (Georgakilas et al., 2012). Graphene is typically synthesized by mechanical cleavage or chemical methods (Guo and Dong, 2011). Particularly, using graphene oxides (GO) as the starting material to produce graphene provides an economic and efficient method for bulk production (Chen et al., 2012). GO can be well-dispersed in aqueous solution due to a rich variety of surface defects and abundant hydrophilic groups on its surface, such as hydroxyl, epoxide and carboxylic groups. As a novel fascinating material, graphene or GO shows many advantages, such as large specific surface area, excellent thermal conductivity, high electrical mobility, great mechanical strength, and low production cost, which

has been widely used in synthesizing nanocomposites and fabricating microelectrical devices (Chung et al., 2013). Recently, GO which can be easily modified has been actively pursued in biotechnology (Huang et al., 2013; Parlak et al., 2013). For example, GO based magnetic composites have been used for drug delivery, biomedical engineering, and biomolecules detection (Shen et al., 2010; Yang et al., 2011, 2009). Moreover, noncovalent functionalization make GO as a perfect substrate to support molecular with improved catalytic activity and stability (Yang et al., 2010). The deposition of porphyrin on GO was achieved through π – π stacking interaction, which can take advantage of both superior properties of GO and the functionalizing molecules (Xu et al., 2009). As the active center of heme-protein, hemin (iron protoporphyrin) has been reported to conjugate with GO to act as a highly active biomimetic oxidation catalyst for bioassay (Deng et al., 2013; Guo et al., 2011; Xue et al., 2012).

Low molecular weight thiols are widely distributed in tissues and cells, which play a significant role in metabolism and cellular homeostasis (Zhang et al., 2004). Tripeptide glutathione (γ -L-glutamyl-L-cysteinylglycine, GSH), the most predominant and abundant cellular thiol, plays a crucial role in living organisms which can be found within human cellular system (Hwang et al.,

* Corresponding author at: Shandong Provincial Key Laboratory of Detection Technology of Tumor Markers, School of Chemistry and Chemical Engineering, Linyi University, Linyi 276005, China. Tel./fax: +86 539 8766867.

E-mail address: bisai11@126.com (S. Bi).

1992; Yi et al., 2009). The reduced form, GSH, can be rapidly oxidized to its dimeric form GSSG in response to oxidative stress within cells (McMahon and Gunnlaugsson, 2012). Therefore, the altered level of intracellular GSH or the GSH/GSSG ratio has become an important indicator in monitoring the overall health of cells and their ability to protect cells against oxidative damage. So far, various analytical methods have been developed for the detection of thiols and thiol-containing peptides, including HPLC (Amarnath et al., 2003), mass spectrometry (Huang and Chang, 2007), electrochemical assay (Pacsial-Ong et al., 2006; Wang et al., 2008), and optical sensor (Wei et al., 2013a, 2013b; Yang et al., 2013; Zong et al., 2013). Recently, fluorescent probes containing S–S bond or Se–N bond were successfully synthesized for determination and imaging of cellular thiols with high sensitivity and selectivity (Pires and Chmielewski, 2008; Tang et al., 2007; Wen et al., 2011). However, these probes were often suffered from complicated synthesis and purification, high cost, photobleaching, and nonspecific signals caused by light excitation. Alternatively, design of simple and sensitive probe for thiols detection still needs to be developed. Moreover, example of convenient and accurate colorimetric method for thiols detection has been scarce reported (Liu et al., 2013; Ma et al., 2012; Yuan et al., 2013). In this assay, magnetic graphene oxide–hemin probes containing disulfide bonds are simply and effectively synthesized for colorimetric detection of thiols in vitro and in the extracts of Ramos cells with high sensitivity.

2. Experimental

2.1. Chemicals and apparatus

Glutathione (GSH) was purchased from Solarbio Co., Ltd (Beijing, China). Graphene oxide (GO) was obtained from Beijing DK Nano Technology Co., Ltd. (China). S-2-pyridylthio cysteamine hydrochloride was purchased from Toronto Research Chemicals Inc. (Canada). Hemin, 2,2'-azino-bis(3-ethylbenzothiazoline-6-sulfonic acid) disodium salt (ABTS²⁻), 2-[4-(2-hydroxyethyl)-1-piperazinyl]ethanesulfonic acid (HEPES) were ordered from Aladdin Chemistry Co. Ltd (China). Thiol modified magnetic particles (MPs) (3–4 μm) were obtained from BaseLine ChromTech Research

Centre (Tianjin, China). Double-distilled, deionized ultrapure water was used in all experiments. All reagents were of analytical grade and used without further purification.

2.2. Preparation of MP-GO–hemin composites

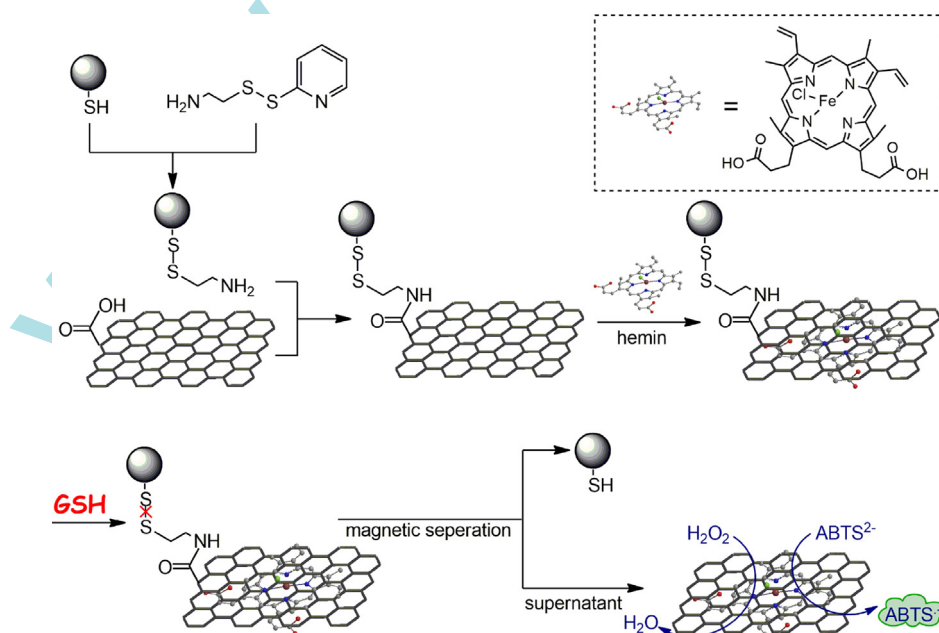
First, 50 μL of thiol-modified MPs were reacted with 100 μL of S-2-pyridylthio cysteamine hydrochloride solution for 2 h, which were washed with 0.01 M PBS buffer (pH 8.0) twice for further use. At the same time, 200 μL of GO suspension (450 μg/mL) was activated by 2 μL of EDC (400 μg/mL) and 2 μL of NHS (320 μg/mL) for 1 h. And then, the –COOH activated GO was added to the above –NH₂-coated MPs, followed by incubation overnight with gentle shaking at room temperature. Finally, 1 mL of hemin-methanol solution (5.0 μM) was added. The mixture was stirred mildly for 3 h to allow the conjugation between hemin and GO. The resulting MP-GO–hemin composites were magnetically washed three times with 0.01 PBS and then re-dispersed in Tris buffer (pH 7.4).

2.3. Characterization

Fourier transform infrared (FT-IR) spectra were performed on a Bruker Tensor 27 FT-IR spectrometer (Bruker Optics, Inc., Billerica, MA). Scan electron microscopy (SEM) and atomic force microscopy (AFM) images were collected on a JSM-6700F microscope (HITACHI, Japan) and a Benyuan Nano-Instruments CSPM-5500 (Beijing, China), respectively. Raman spectra were conducted with a Renisaw Invia Raman spectrometer RamLab-010. The UV–Vis absorbance measurements were performed on a Cary 50 UV–Vis spectrophotometer (Varian, USA).

2.4. GSH assay

A 800 μL of different concentration of GSH in 0.01 M PBS buffer (pH 7.0) was added to the above prepared MP-GO–hemin composites. After reaction for 30 min at 25 °C in dark, the suspension and washings from MPs were combined through magnetic separation to a total volume of 1 mL. The resulting solution containing the released GO–hemin conjugates was reacted with 400 μL of ABTS²⁻ (10 mM), 600 μL of H₂O₂ (7.5 mM) in a buffer solution consisting of



Scheme 1. Fabrication of MP-GO–hemin probe containing disulfide bonds for GSH detection.

HEPES (25 mM), KCl (20 mM) and NaCl (200 mM) (pH 7.4) at 25 °C for 20 min. The UV–Vis absorbance was recorded in the wavelength from 390 nm to 480 nm. For the detection of intracellular thiols in the extracts of Ramos cells, the samples were prepared according to Tang et al. (2007)'s work, which were analyzed as described above.

3. Results and discussion

3.1. Principle of the assay

In this assay, a novel MP-GO-hemin probe containing a disulfide bond is effectively synthesized through amide reaction to covalently link magnetic particles to GO surface and π - π stacking interaction between hemin and GO to immobilize hemin on GO, which is successfully applied to colorimetric detection of thiols by using GSH as a model analyte. Scheme 1 depicts the fabrication of magnetic particle (MP)-GO, the immobilization of hemin on GO, and the colorimetric analysis of GSH. First, thiol-modified MPs are treated with S-2-pyridylthio cysteamine hydrochloride to obtain functionalized MPs with disulfide bonds and amino group at the end. At the same time, GO is activated with EDC and NHS, whose carboxylic groups are further reacted with the amino groups of the as-prepared MPs to synthesize the MP-GO conjugates. Then hemin is immobilized on the surface of GO through π - π stacking interactions. The excess hemin can be easily removed through magnetic separation. In the presence of GSH, the disulfide bonds can be reduced and cleaved, resulting in the release of GO-hemin from MPs to solution. After magnetic separation, the supernatant containing the released GO-hemin composites have the intrinsic peroxidase-like activity that can catalyze the oxidation of 2,2'-azino-bis(3-ethylbenzothiazoline)-6-sulfonic acid (ABTS²⁻) by H₂O₂ to produce the colored ABTS^{•+}, thus providing an amplified colorimetric readout signal for the detection of GSH. In comparison with other methods for thiols detection, the major advantage of the proposed strategy is that the magnetic probes can significantly facilitate the preparation. During the fabrication and purification procedures, the excess GO and hemin can be easily removed by magnetic separation. In addition, the large surface area-to-volume ratio of MPs provides high binding capacity, which enhances the assay sensitivity. Moreover, the magnetic probe can significantly simplify the analysis procedures. After reaction with thiols, the released GO-hemin hybrids can be easily collected via magnetic field. Thus, MPs used in the present strategy play important roles in not only simplifying the experimental operation but also increasing the sensing efficiency. In addition, this method has the advantage of rapidity. After fabricating the MP-GO-hemin probe, it takes only 30 min to reaction with samples and 20 min to UV–Vis measurement.

3.2. Characterization of MP-GO composites

The SEM is used to investigate the morphology characteristics of GO and MP-GO conjugates. From Fig. 1a, the unmodified GO displays a wrinkle paper-like structure that has a smooth surface without any folds, indicating its good solubility. After the deposition of MPs on GO through amide reaction ($-\text{COOH}$ group on GO and $-\text{NH}_2$ group on MPs), SEM image shows that MPs are loaded on a part of GO due to the large specific surface area of GO (Fig. 1b). In addition, the introduction of MPs into the dispersion of GO sheets inhibits the formation of a stacked graphitic structure. As a functional "spacer", MPs increase the distance between the graphene sheets, which ensure both faces of GO are accessible to further immobilize hemin and the high specific surface area of MPs is remained (Shen et al., 2010). As a powerful and nondestructive tool to characterize carbonaceous materials, Raman spectra are also applied to investigate GO and the formation of MP-GO conjugates. As shown in Fig. 1, the Raman spectrum of GO displays two peaks at $\sim 1594\text{ cm}^{-1}$ and $\sim 1350\text{ cm}^{-1}$, which is corresponded to the vibration of the sp^2 -bonded carbon atoms (G band) and vibration of carbon atoms with dangling bonds in plane terminations of disordered graphite (D band), respectively (Jiang et al., 2012; Wei et al., 2013a,2013b). After the formation of MP-GO composites, the intensity ratio of D over G band (I_D/I_G) (0.87) is lower than that of GO (0.99), indicating that more sp^2 domains are formed during the conjugation. Therefore, the MP-GO composites are successfully synthesized as expected.

3.3. Characterization of hemin-functionalized GO and its conjugation with MPs

The morphology and thickness of GO and hemin-functionalized GO are investigated by AFM studies. GO aqueous solution is first deposited onto a mica substrate from an aqueous solution to determine the thickness of the selected GO flakes, which is then immersed into the hemin-methanol solution to ensure the absorption of hemin on GO. From Fig. 2a, the height of GO sheets is $\sim 0.73\text{ nm}$, which is comparable to that of typical monolayer well-exfoliated graphene sheets (Guo et al., 2011). After absorption of hemin, AFM studies show that the mean thickness of the same GO flakes is determined to be $\sim 1.27\text{ nm}$ (Fig. 2b). In comparison with the unmodified GO, the $\sim 0.54\text{ nm}$ increment in the thickness can be attributed to the functionalization of hemin on GO sheet surfaces. Since the thickness of a single hemin molecular is 0.2 nm and hemin could be located on both sides of the GO layer, it is reasonable to suggest that a monolayer of hemin molecules adsorbs onto GO sheet (Guo et al., 2011; Xue et al., 2012).

The successful synthesis of GO-hemin conjugates is also confirmed by UV–Vis spectra (Fig. 2c). For the GO dispersion (curve a), the maximum absorption at 230 nm is assigned to the π - π^* transition of the aromatic C=C bonds and the shoulder at 290–300 nm is

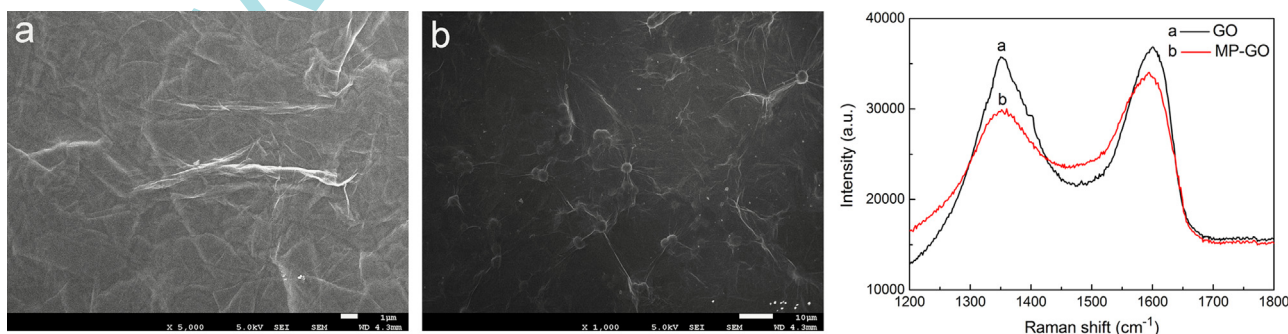


Fig. 1. SEM and Raman spectra of (a) GO and (b) MP-GO composites.

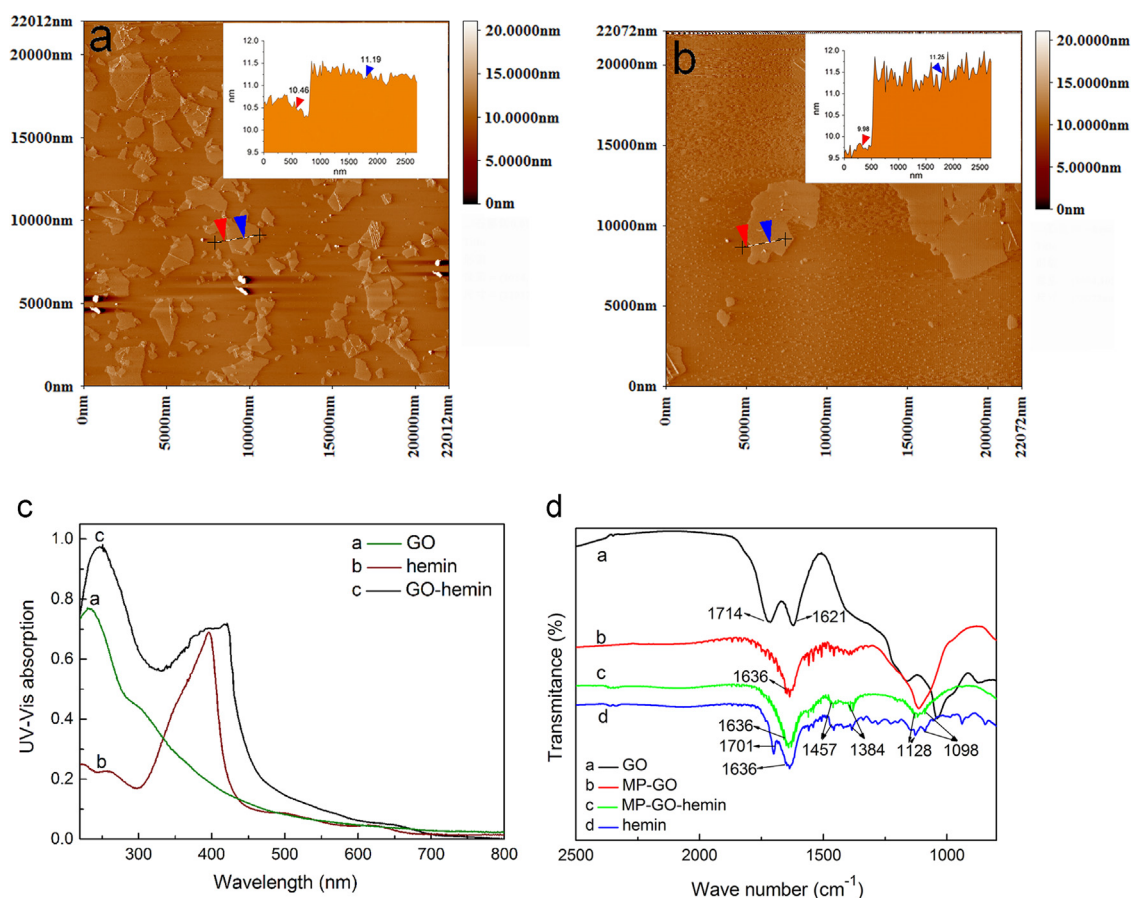


Fig. 2. AFM morphology of (a) GO and (b) GO-hemin conjugates. Inset: the profile analysis of the heights indicated by the arrows. (c) UV-Vis absorption spectra of GO dispersion, hemin solution, and GO-hemin suspension. (d) FT-IR spectra of GO, MP-GO, MP-GO-hemin, and hemin.

corresponded to the $n-\pi^*$ transition of C=O bond. For hemin solution (curve *b*), a strong absorption peak at 396 nm and a group of weak peaks between 500 nm and 700 nm are attributed to the Soret band and Q-bands, respectively. The GO-hemin suspension (curve *c*) displays a broad absorption at 251 nm that should be the corresponding GO. In addition, in comparison with the Soret band of free hemin solution, a stronger band at 421 nm is also observed, which is assigned to the Soret band of hemin that undergoes a large bathochromic shift of 25 nm. All these results indicate the existence of the $\pi-\pi$ interactions between GO and hemin and strongly confirm that hemin molecules are successfully attached onto GO surface (Guo et al., 2011; Xue et al., 2012). Moreover, FT-IR spectra are used to characterize the fabrication of MP-GO-hemin conjugates (Fig. 2d). As shown in curve *a*, the peak at 1714 cm^{-1} is corresponding to C=O stretch of -COOH on GO surface, which disappears with the appearance of a new characteristic peak at 1636 cm^{-1} due to the formation of -COO⁻ after interacting with NH₂-MPs (curve *b*), implying that MPs are covalently linked to GO surface via amide reaction (Jiang et al., 2012). After further reacting with hemin to form the MP-GO-hemin conjugates (curve *c*), the characteristic peaks of hemin (curve *d*) can be observed, confirming the successful immobilization of hemin on GO.

3.4. Optimization of conditions

The influences of the working pH, the concentration of hemin in GO, the incubation time and the reaction temperature on GSH detection were investigated. As shown in Fig. 3a, GSH was dissolved to a series of PBS buffers with pH from 5.5 to 9.0 to a concentration of 1.0×10^{-8} M, which then reacted with solid

MP-GO-hemin probe. The relative UV-Vis absorbance increases when pH ranges from 5.5 to 7.0, which then decreased from 7.4. Therefore, the PBS with pH 7.0 was selected for the best UV-Vis response on the reaction of MP-GO-hemin and GSH. In addition, the concentration of hemin to fabricate MP-GO-hemin probe was investigated. From the results of Fig. 3b, for the detection of 1.0×10^{-8} M GSH, as the concentration of hemin increases from 0.1 to 5.0 μM the relative UV-Vis absorption increases, which almost reaches saturation from 5.0 μM . Thus, we use 5.0 μM hemin to prepare the MP-GO-hemin conjugates.

From Fig. 3c, after the treatment of 1.0×10^{-8} M GSH with the fabricated MP-GO-hemin probe for 0 min, 10 min, 20 min, 30 min, 1 h, 2 h, and 3 h at 25 °C in dark, respectively, the UV-Vis signal increase with reaction time and then levels off from 30 min. Thus, 30 min was selected as the optimum incubation time for GSH detection. Moreover, a series of temperature-changing assays were carried out in the absence and presence of 1.0×10^{-8} M GSH for 30 min at 25 °C, 37 °C, 45 °C, and 60 °C in dark, respectively. As observed from Fig. 3d, the optimum temperature occurs at 25 °C, which could be attributed to the stability of GSH.

3.5. Effect of GO and GSH on the UV-Vis system

It has been reported that GO has an intrinsic peroxidase-like activity, which is strongly dependent on pH, temperature, and H₂O₂ concentration (Qu et al., 2011; Song et al., 2010; Sun et al., 2013). For example, GO can catalyze the reaction of peroxidase substrate 3,3',5,5'-tetramethylbenzidine (TMB), in the presence of H₂O₂ to produce a colorimetric signal under the optimum conditions of pH 4.0 at 35 °C and 150 mM H₂O₂ (Song et al., 2010). In our

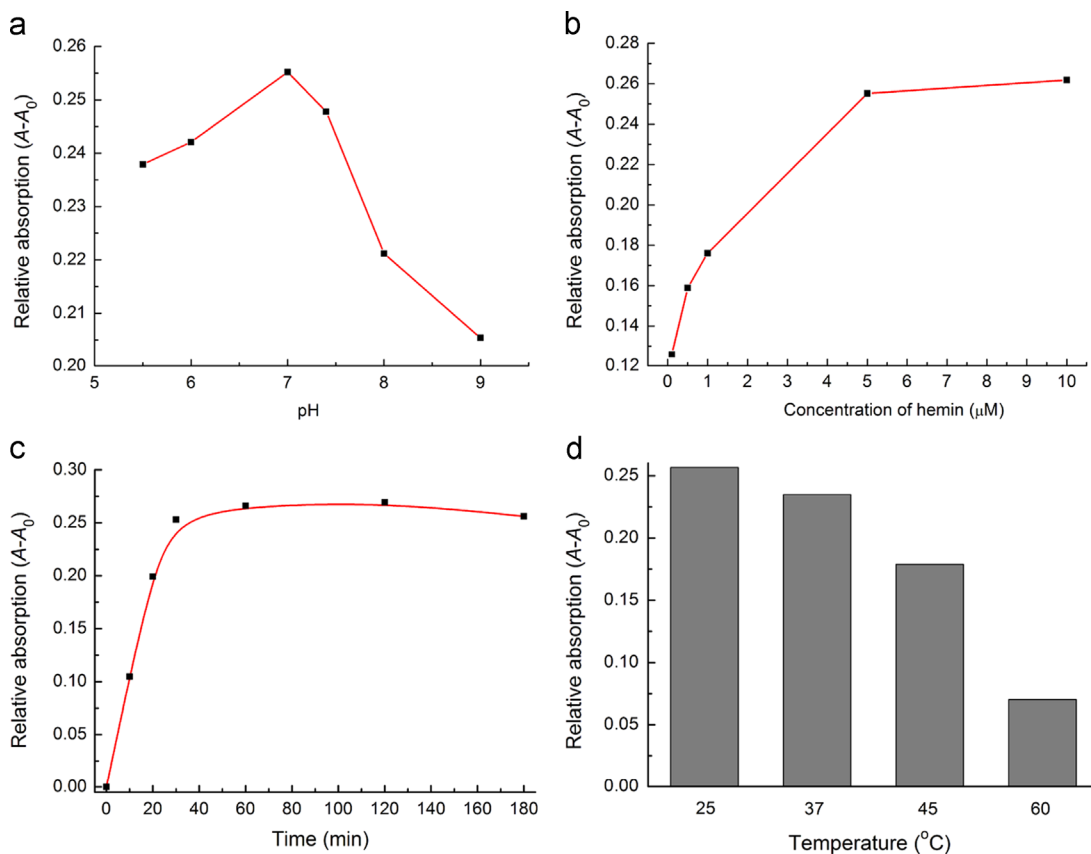


Fig. 3. The influences of (a) pH, (b) the concentration of hemin to fabricate MP-GO-hemin probe, (c) incubation time and (d) reaction temperature on GSH detection. The concentration of GSH is 1.0×10^{-8} M. The other conditions are the same as those in Section 2.

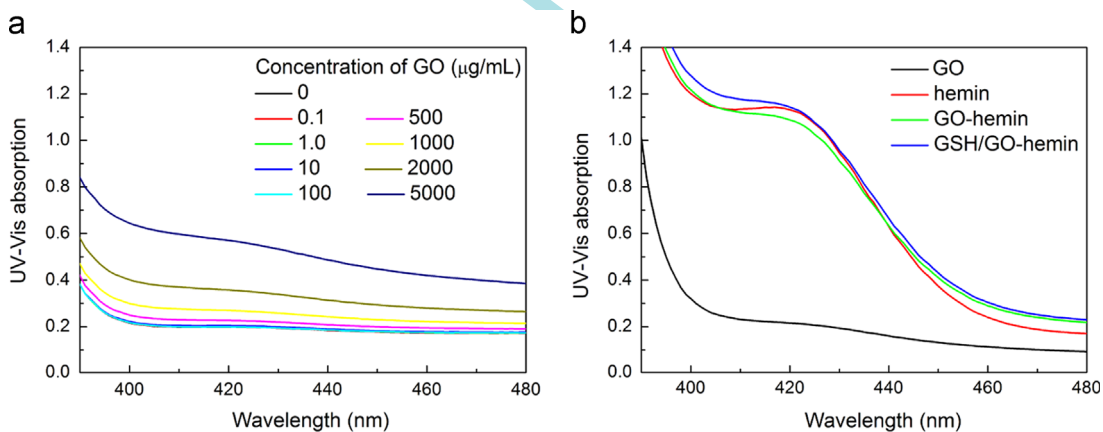


Fig. 4. UV-Vis spectra in response to the ABTS^{2-} - H_2O_2 system reacted with (a) different concentrations of GO, and (b) GO, hemin, GO-hemin, and GSH/GO-hemin with the same concentrations of each component (GO, 450 $\mu\text{g}/\text{mL}$; hemin, 5.0 μM ; GSH, 1.0 μM). The conditions of ABTS^{2-} - H_2O_2 detection system are the same as that in Section 2.

assay for the ABTS^{2-} - H_2O_2 -hemin detection system, the pH, temperature, and H_2O_2 concentration are pH 7.4, 25 °C, and 7.5 mM, respectively. Under these conditions, a range of GO concentrations from 0.1 $\mu\text{g}/\text{mL}$ to 5 mg/mL were tested (Fig. 4a). For the fabrication of MP-GO-hemin conjugates, the concentration of GO is 450 $\mu\text{g}/\text{mL}$. Thus, it can be seen that GO has no influence on this assay. In addition, the samples of GO, hemin, GO-hemin, and GSH/GO-hemin at the same concentrations of each component (GO, 450 $\mu\text{g}/\text{mL}$; hemin, 5.0 μM ; GSH, 1.0 μM) were detected by ABTS^{2-} - H_2O_2 system (Fig. 4b). Even the concentration of GSH as high as 1.0 μM , the UV-Vis signal induced by GSH/GO-hemin is comparable to that of GO-hemin or free hemin, indicating that GSH has no influence on the UV-Vis detection system.

3.6. Sensitive and specific detection of GSH

After investigating GO and GSH have no influence on the ABTS^{2-} - H_2O_2 UV-Vis detection system and optimizing the experimental conditions, the prepared MP-GO-hemin probe is applied to GSH analysis by colorimetric technology. After treating the hemin-GO-MPs with different concentrations of GSH for 30 min, the suspension and washings containing the released GO-hemin conjugates are collected by magnetic separation, which are then subjected to UV-Vis detection. As shown in the UV-Vis spectra (Fig. 5a), the maximum absorption wavelength of the colored product ABTS^- is seen at ~ 419 nm, which is used for quantitative analysis of GSH. As the concentration of GSH increases, the UV-Vis signal increases

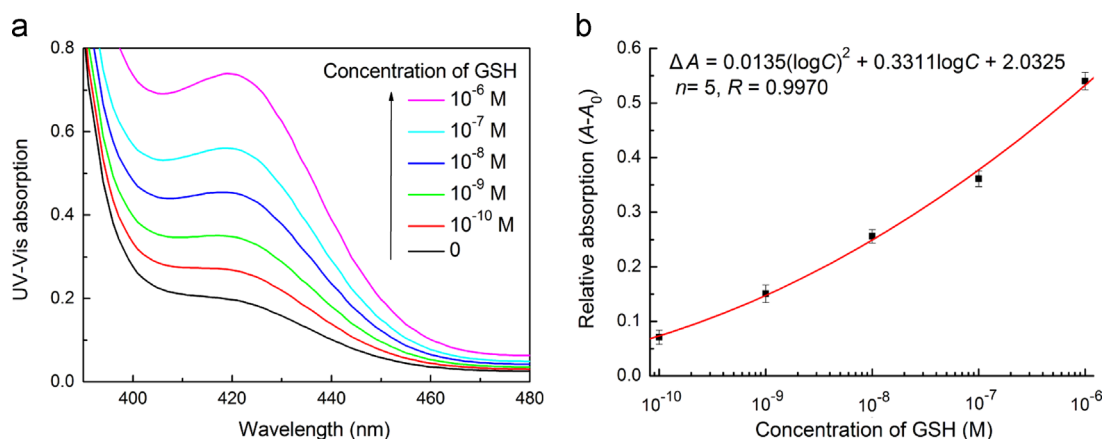


Fig. 5. (a) UV-Vis spectra in response to different concentrations of GSH: 0 M, 10^{-10} M, 10^{-9} M, 10^{-8} M, 10^{-7} M, 10^{-6} M. (b) Corresponding calibration curve of the relative UV-Vis absorbance (ΔA) versus various concentrations of GSH. ΔA is calculated by $A-A_0$, where A_0 and A are the UV-Vis absorbance without and with target GSH, respectively. The error bars represent the standard deviation for three replicates.

correspondingly. The relationship between relative UV-Vis absorbance (ΔA) and concentrations of GSH in logarithmic scales is obtained with the GSH concentration changed in the range from 1.0×10^{-10} M to 1.0×10^{-6} M (Fig. 5b). ΔA is calculated by $A-A_0$, where A_0 and A are the UV-Vis absorbance without and with target GSH, respectively. It should be noted that it has been reported that the coverage of hemin on GO is 19–20% (Guo et al., 2011; Song et al., 2013). Thus, it cannot be simply considered that each GSH molecular liberates a hemin molecular to show a linear relationship between GSH concentration and relative UV-Vis absorbance. The kinetic of hemin catalyzed colorimetric system for bioanalytes detection is similar to the reported works (Tao et al., 2013; Teller et al., 2009; Weizmann et al., 2006). The regression equation is expressed as $\Delta A = 0.0135(\log C)^2 + 0.3311 \log C + 2.0325$ with a correlation coefficient (R^2) of 0.9970 ($n=5$). The limit of detection (LOD) was calculated to be 8.1×10^{-11} M by using 3σ criterion (the slope of linear calibration curve was obtained when the concentration of GSH from 1.0×10^{-10} M to 1.0×10^{-7} M), which is more sensitive than or comparable to other related sensors for GSH detection (Table S1). To investigate the in vitro stability of the MP-GO-hemin probe, after stored at 4°C for one month, the UV-Vis signal obtained by measuring 1.0×10^{-9} M GSH is similar to that obtained by freshly fabricated probes. In addition, the relative standard deviation (RSD) obtained by 1.0×10^{-9} M GSH is 4.2% for seven measurements, indicating the good stability and reproducibility of the fabricated probe for GSH assay.

The effect of diverse biorelevant analytes on GSH detection is further investigated for control experiments. It has been reported that metal ions, macro-like metal (such as Mg^{2+} , Ca^{2+} , K^+ , Na^+) and trace-like metal (such as Zn^{2+} , Cu^{2+} , Fe^{3+} , Cd^{2+}) widely exist in cell, tissue, and body fluid, which play important roles in human physiology and pathology (Fan et al., 2012; Luo et al., 2003). In order to demonstrate the practicability of prepared MP-GO-hemin probe for GSH detection in real sample assay, the effect of diverse biorelevant analytes including metal ions, bioamines, and biological antioxidants is investigated on GSH detection. From the results of Fig. S1, in comparison with the UV-Vis signal generated by GSH, the interferences can be ignored when the synthesized probe is used to detect other analytes. Thus, the proposed assay successfully accomplishes qualitative, quantitative and selective detection of GSH.

In addition, the reactivity of the prepared MP-GO-hemin probe with thiol-containing analytes is investigated, showing that the MP-GO-hemin probe containing disulfide bonds is more sensitive to protein thiols than non-protein thiols. To further evaluate the applicability of this method in clinical analysis, intracellular non-

protein thiols and protein thiols in the extracts of Ramos cells (human Burkitt's lymphoma cells) are examined. It has been demonstrated that there is no cell cytotoxicity of MP-GO-hemin on cells for intracellular thiols detection. The thiols concentrations in 10^4 Ramos cells obtained by the present method are in good agreement with those determined by electrochemical method (Wang et al., 2008) with the relative deviation of 7.4% for non-protein thiols detection and 4.5% for protein thiols detection, indicating our detection method compares favorably with electrochemical method for the detection of thiols in the extracts of Ramos cells. In addition, the MP-GO-hemin probe can detect non-protein thiols in Ramos extracts as low as 500 cells (see supporting information for details).

4. Conclusion

In summary, a novel MP-GO-hemin probe containing a disulfide bond is developed for the analysis of thiols in vitro and in the extracts of Ramos cells. On the basis of π - π stacking interaction between hemin and GO to fabricate the peroxidase probe and strong nucleophilicity of sulfhydryl to cleave S-S bond, the proposed strategy achieves the detection of standard solution of GSH in the linear range from 1.0×10^{-10} M to 1.0×10^{-6} M with a detection limit of 8.2×10^{-11} M (3σ) and good specificity. Significantly, the new probe is successfully applied to non-protein thiols and protein thiols detection in extracts of Ramos cells as low as 500 cells. This assay is easy operation and cost-effective, which not only offers a new technique for thiols detection, but also opens a new field for the application of graphene in biotechnology, biosensors and medicine.

Acknowledgements

This work was supported by the National Science Foundation of China (21375056 and 21105052), the Program for New Century Excellent Talents in University of Ministry of Education of China (NCET-12-1024), the Natural Science Foundation of Shandong province (no. ZR2011BQ025).

Appendix A. Supporting information

Supplementary data associated with this article can be found in the online version at <http://dx.doi.org/10.1016/j.bios.2014.01.025>.

References

- Amarnath, K., Amarnath, V., Amarnath, K., Valentine, H.L., Valentine, W.M., 2003. *Talanta* 60, 1229–1238.
- Chen, D., Feng, H., Li, J., 2012. *Chem. Rev.* 112, 6027–6053.
- Chung, C., Kim, Y.-K., Shin, D., Ryoo, S.-R., Hong, B.H., Min, D.-H., 2013. *Acc. Chem. Res.* 46, 2211–2224.
- Deng, S., Lei, J., Huang, Y., Cheng, Y., Ju, H., 2013. *Anal. Chem.* 85, 5390–5396.
- Fan, W.-Z., Ma, J., Chen, J.-P., Lin, L.-R., Huang, R.-B., 2012. *Chem. Reag.* 34, 673–684.
- Georgakilas, V., Otyepka, M., Bourlinos, A.B., Chandra, V., Kim, N., Kemp, K.C., Hobza, P., Zboril, R., Kim, K.S., 2012. *Chem. Rev.* 112, 6156–6214.
- Guo, S., Dong, S., 2011. *Chem. Soc. Rev.* 40, 2644–2672.
- Guo, Y., Deng, L., Li, J., Guo, S., Wang, E., Dong, S., 2011. *ACS Nano* 5, 1282–1290.
- Huang, J., Zhang, L., Liang, R.-P., Qiu, J.-D., 2013. *Biosens. Bioelectron.* 41, 430–435.
- Huang, Y.-F., Chang, H.-T., 2007. *Anal. Chem.* 79, 4852–4859.
- Hwang, C., Sinskey, A.J., Lodish, H.F., 1992. *Science* 257, 1496–1502.
- Jiang, B., Yang, K., Zhao, Q., Wu, Q., Liang, Z., Zhang, L., Peng, X., Zhang, Y., 2012. *J. Chromatogr. A* 1254, 8–13.
- Liu, X., Wang, Q., Zhang, Y., Zhang, L., Su, Y., Lv, Y., 2013. *New J. Chem.* 37, 2174–2178.
- Luo, Q., Wang, J.-H., Wang, Y.-L., Pan, 2003. *J. Chongqing Univ.* 26, 97–101.
- Ma, Y., Zhang, Z., Ren, C., Liu, G., Chen, X., 2012. *Analyst* 137, 485–489.
- McMahon, B.K., Gunnlaugsson, T., 2012. *J. Am. Chem. Soc.* 134, 10725–10728.
- Pacsial-Ong, E.J., McCarley, R.L., Wang, W., Strongin, R.M., 2006. *Anal. Chem.* 78, 7577–7581.
- Parlak, O., Tiwari, A., Turner, A.P.F., Tiwari, A., 2013. *Biosens. Bioelectron.* 49, 53–62.
- Pires, M.M., Chmielewski, J., 2008. *Org. Lett.* 10, 837–840.
- Qu, F., Li, T., Yang, M., 2011. *Biosens. Bioelectron.* 26, 3927–3931.
- Shen, J., Hu, Y., Shi, M., Li, N., Ma, H., Ye, M., 2010. *J. Phys. Chem. C* 114, 1498–1503.
- Song, Y., Qu, K., Zhao, C., Ren, J., Qu, X., 2010. *Adv. Mater.* 22, 2206–2210.
- Song, H., Ni, Y., Kokot, S., 2013. *Anal. Chim. Acta* 788, 24–31.
- Sun, W., Ju, X., Zhang, Y., Sun, X., Li, G., Sun, Z., 2013. *Electrochem. Commun.* 26, 113–116.
- Tang, B., Xing, Y., Li, P., Zhang, N., Yu, F., Yang, G., 2007. *J. Am. Chem. Soc.* 129, 11666–11667.
- Tao, Y., Lin, Y., Ren, J., Qu, X., 2013. *Biomaterials* 34, 4810–4817.
- Teller, C., Shimron, S., Willner, I., 2009. *Anal. Chem.* 81, 9114–9119.
- Wang, W., Li, L., Liu, S., Ma, C., Zhang, S., 2008. *J. Am. Chem. Soc.* 130, 10846–10847.
- Wei, M., Yin, P., Shen, Y., Zhang, L., Deng, J., Xue, S., Li, H., Guo, B., Zhang, Y., Yao, S., 2013a. *Chem. Commun.* 49, 4640–4642.
- Wei, W., Zhang, D.M., Yin, L.H., Pu, Y.P., Liu, S.Q., 2013b. *Spectrochim. Acta, Part A* 106, 163–169.
- Weizmann, Y., Beissenhertz, M.K., Cheglakov, Z., Nowarski, R., Kotler, M., Willner, I., 2006. *Angew. Chem. Int. Ed.* 45, 7384–7388.
- Wen, H.-Y., Dong, H.-Q., Xie, W.-J., Li, Y.-Y., Wang, K., Pauletti, G.M., Shi, D.-L., 2011. *Chem. Commun.* 47, 3550–3552.
- Xu, Y., Zhao, L., Bai, H., Hong, W., Li, C., Shi, G., 2009. *J. Am. Chem. Soc.* 131, 13490–13497.
- Xue, T., Jiang, S., Qu, Y., Su, Q., Cheng, R., Dubin, S., Chiu, C.-Y., Kaner, R., Huang, Y., Duan, X., 2012. *Angew. Chem. Int. Ed.* 51, 3822–3825.
- Yang, H., Zhang, Q., Shan, C., Li, F., Han, D., Niu, L., 2010. *Langmuir* 26, 6708–6712.
- Yang, X., Wang, Y., Huang, X., Ma, Y., Huang, Y., Yang, R., Duan, H., Chen, Y., 2011. *J. Mater. Chem.* 21, 3448–3454.
- Yang, X., Zhang, X., Ma, Y., Huang, Y., Wang, Y., Chen, Y., 2009. *J. Mater. Chem.* 19, 2710–2714.
- Yang, Y., Huo, F., Yin, C., Zheng, A., Chao, J., Li, Y., Nie, Z., Martínez-Mañez, R., Liu, D., 2013. *Biosens. Bioelectron.* 47, 300–306.
- Yi, L., Li, H., Sun, L., Liu, L., Zhang, C., Xi, Z., 2009. *Angew. Chem. Int. Ed.* 48, 4034–4037.
- Yuan, Y., Zhang, J., Wang, M., Mei, B., Guan, Y., Liang, G., 2013. *Anal. Chem.* 85, 1280–1284.
- Zhang, S., Ong, C.-N., Shen, H.-M., 2004. *Cancer Lett.* 208, 143–153.
- Zong, S., Wang, Z., Chen, H., Yang, J., Cui, Y., 2013. *Anal. Chem.* 85, 2223–2230.